sciendo

DOI: 10.2478/awutp-2018-0007

ANNALS OF WEST UNIVERSITY OF TIMISOARA PHYSICS
Vol. LX, 2018

EFFECT OF Cu_2O MORPHOLOGY ON PHOTOVOLTAIC PERFORMANCE OF P-TYPE DYE-SENSITIZED SOLAR CELLS

Daniel Ursu[1], Anamaria Dabici[1], Melinda Vajda[1], Neli-Camelia Bublea[1], Narcis Duteanu[2], Marinela Miclau[1] *

[1] *National Institute for Research and Development in Electrochemistry and Condensed Matter, Dr. A. Păunescu-Podeanu Street 144, 300569 Timisoara, Romania*

[2] *Politehnica University Timisoara, Str. PiataVictoriei, nr.2, 300006 Timisoara, Romania*

Article Info	Abstract
Received: 10.03.2018 *Accepted: 14.06.2018* **Keywords:** p-type dye-sensitized solar cell; cuprous oxide; hydrothermal method.	Cuprous oxide with different morphologies (3D hierarchical structure consisting of the micrometer dendritic rods and the porous truncated octahedrons) has been successfully synthesized via a facile one-step hydrothermal method using copper (II) acetate and ethyl cellulose as reactants. The p-type dye-sensitized solar cell based on the micrometer porous structure exhibits approximately 15% increase in J_{SC} and V_{OC} than 3D hierarchical structure. This enhancement could be explained by the high dye loading capacity of this porous structure and lowering the recombination process at the oxide/dye/electrolyte interface.

1. Introduction

Mimicking the natural photosynthesis, the dye-sensitized solar cell (DSSC), 3rd generation solar cell, attracts great research interests because of low manufacturing cost and environmentally friendly character. The concept of DSSC was proposed by Gratzel and co-workers, being validated by the good conversion efficiencies of n-DSSCs (efficiencies up to 13%) based on TiO_2 and organic solvent-based liquid electrolytes [1].

In p-type dye-sensitized solar cells (p-DSSCs), NiO is the most commonly used p-type semiconductor [2]. Considering the drawbacks of NiO, alternative p-type semiconductors with better optical transparency, lower VB edge position and higher hole mobility are desired for p-DSSCs [3]. The cuprous oxide (Cu_2O) is a natively p-type semiconductor with a direct band gap of about 1.9–2.2 eV [4]. It's non-toxic nature, the stability, natural abundance, low cost production, good electrical properties and a good absorption coefficient for visible light

prompted to investigate the cuprous oxide as a material suitable for the realization of low cost and large scale p-DSSCs [5]. The nanoparticles have been intensively studied as photocathodes materials for DSSCs because of their larger specific surface areas to absorb more dye molecules. At the same time, the small-sized particles have shown low scattering of the solar radiation reducing the light-harvesting efficiency. Based on these premises, we propose to investigate the effect of micrometer-size structures on the photovoltaic performance of p-DSSCs based on cuprous oxide.

In this work, 3D hierarchical structure built of the micrometer dendritic rods and the porous truncated octahedrons have been successfully synthesized via a facile one-step hydrothermal method using copper (II) acetate and ethyl cellulose as reactants. The DSSC based on the porous structure exhibits approximately 15% increase in J_{SC} and V_{OC} than 3D hierarchical structure.

2. Method and samples

2.1. Synthesis of Cu_2O powder

In typical synthesis process, copper (II) acetate and ethyl cellulose (1.2g) were mixed in 30 ml of water. The Cu_2O_1 and Cu_2O_2 were prepared using 2.4 g and 1.2 g of copper (II) acetate, respectively. The obtained solution was transferred into Teflon-line autoclave with a volume of 60 mL. The copper plate with 12.5 x 12.5 x 0.5 mm and with 99% purity washed with 0.1 M HCl for 10 minutes and the ultrasonic cleaning in distilled water for 30 minutes was added in the autoclave as metallic copper source. Samples were prepared at 180 °C for 24 h (Cu_2O_1) and 6 h (Cu_2O_2). The autoclave was cooled down to room temperature naturally. The precipitate was filtered and washed with deionized water and then, the product was dried at 80 °C for 1h.

The crystal structure of the prepared samples was characterized by X-ray powder diffraction (XRD) PW 3040/60 X'Pert PRO using Cu-Kα radiation with (λ=1.5418Å), in the range 2θ = 20-80°. The microstructure of copper oxide powder was observed by Scanning Electron Microscope Inspect S (SEM). The diffuse reflectance spectra (DSR) was obtained using a Lambda 950 UV-Vis-NIR Spectrophotometer with 150 mm integrating sphere in the wavelength range of 300–800 nm. All the measurements were performed at room temperature.

The electrochemical investigations were performed using a Voltalab potentiostat model PGZ 402, with VoltaMaster 4 (version 7.09) software. A single compartment three-electrode cell based on a platinum wire as counter electrode, Ag/AgCl/KCl electrode in a

saturated solution of KCl coupled to a Luggin capillary as reference electrode and Cu_2O film as working electrodes (area 0.28 cm^2) was used. In order to obtain working electrode, Cu_2O powder was mixed with 5 wt% polyvinylidene fluoride (PVDF) in N-methyl-2-pyrrolidone. (NMP) solution and the obtained paste was coated on FTO substrate using Doctor- Blade technique and following by the calcinations at 300 **°C.** All potentials were referenced to the standard hydrogen electrode (SHE). The capacitance of the interface was measured using 10^{-1} mol/L Na_2SO_4 aqueous solutions, in the potential range: -0.5 ÷ -0.1 V with a 25 mV potential step at 3.1646 kHz and amplitude of 20 mV ac potential.

2.2. Preparation of Cu_2O and DSSCs

The preparation of Cu_2O_1 and Cu_2O_2 paste had followed a modified procedure obtained from the literature using ethyl cellulose (EC) as binder [6]. 50 mg of the powder was mixed with 0.1mL glacial acetic acid, 0.15mL DI water, 0.075g EC dissolved in 2.5 ml ethanol and 1 ml terpineol and magnetic stirring for 2 hours at a speed of 300 rpm at 50 °C. The resulting Cu_2O_1 and Cu_2O_2 paste with a suitable viscosity was deposited on FTO-coated glass substrate using doctor Blade method and sintered at 100 °C for 1 hour. After annealing under air flow at 340 ºC for 1 h, the photocathode was immersed into a 0.4 mM P1 dye under dark for 24 h. Catalytic counter electrodes were produced by thermal decomposition of H_2PtCl_6 solution on FTO-coated glasses using a hot-wind gun set at 400ºC for 30 minutes. The iodine/tri-iodide electrolyte solution was prepared by adding 1 M BMII, 0.1 M I_2 and 0.2 M of 4-tert-butylpyridine in acetonitrile. The dye-sensitized photocathodes and Pt counter electrode were fixed together using a hot-melt film spacer. The DSSC was assembled by injecting electrolyte into the space between the electrodes. Solar cell performances were recorded on a Digital Multimeter, under AM 1.5G simulated sunlight (100 mW cm^{-2}). Impedance measurements were performed with a potentiostat under dark conditions, at a bias potential of 0.14 V. The frequency range is 0.001–10 kHz and the magnitude of the modulation signal is 10 mV.

3. Results and Discussions

XRD patterns of the Cu_2O_1 and Cu_2O_2 compound, obtained from hydrothermal method are shown in figure 1. All the diffraction peaks could be indexed as Cu_2O (cuprite) with cubic structure (space group: *Pn-3m*; JCPDS Nr. 01-074-1230), only a small amount of CuO is detected as impurity in Cu_2O_2 sample. The formation of CuO phase is determined

by the time reaction which in the case of Cu_2O_2 is still small to establish completely Cu^{+1} oxidation state.

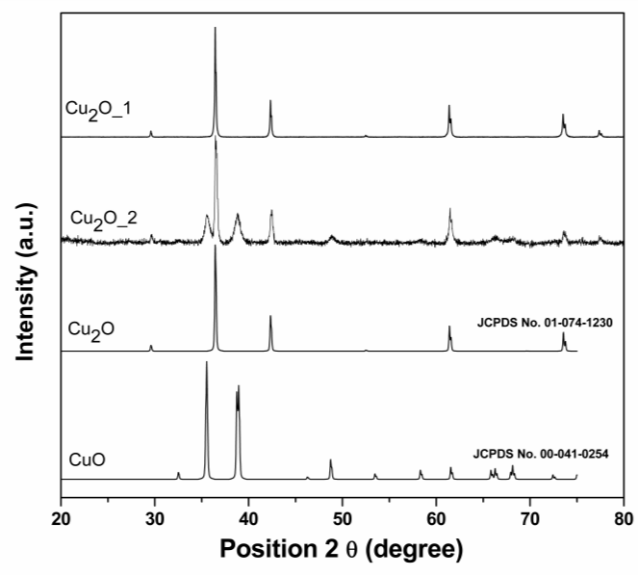

Fig. 1. Room temperature X-ray diffraction patterns of Cu_2O_1 and Cu_2O_2 samples.

The SEM image (figure 2a) of Cu_2O_1 powder shows the 3D hierarchical structure consisting of micrometer dendritic rods. In case of Cu_2O_2 sample, the SEM image (figure 2b) shows that the grains are in the shape of the porous truncated octahedron, partially covered by the microspheres. The diameter of the microspheres is close to the size of the pores, confirming the assumption that the formation of the porous powder could be explained by Ostwald ripening of the microspheres [7]. In both samples, ethyl cellulose plays a key role by tuning the copper oxide morphology from 3D hierarchical structure to the porous structure

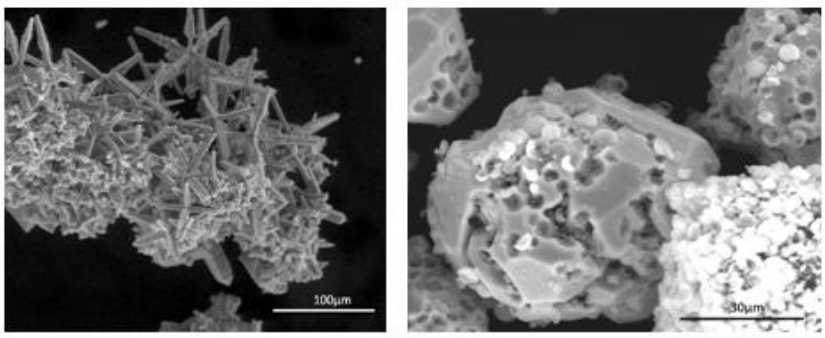

a **b**

Fig. 2. SEM images of Cu_2O_1 (a) and Cu_2O_2 (b) samples.

The optical direct band gap of Cu_2O is estimated by the equation $(\alpha h\nu)^2 = A(h\nu - E_g)$, where α,ν, A and E_g are the absorption coefficient, the frequency of light, a constant and the band gap, respectively [8]. The $(\alpha h\nu)^2$ *vs.* $h\nu$ plot gives the value of optical direct band gap by the extrapolation of the straight line to $(\alpha h\nu)^2 = 0$ axis (Figure 3). It is calculated to 1.91 eV for the Cu_2O_1 sample, 1.75 eV and 1.47 eV for the Cu_2O_2, respectively, the values of Cu_2O and CuO close to the one reported in earlier studies [9].

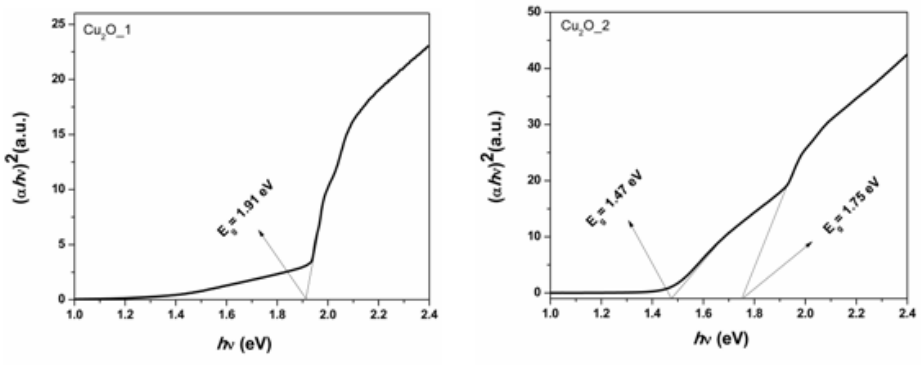

a **b**

Fig. 3. Band gap of Cu_2O_1 (a) and Cu_2O_2 (b) calculated from the reflectance spectrum.

The Mott-Schottky analysis of Cu_2O_1 and Cu_2O_2 are presented in figure 4, where the linear part of the curve is extrapolated to $1/C^2 = 0$ and the values of V_{FB} are estimated to be 0.41 V and 1.27 V. Both samples show negative slopes, in accordance with the expected p-type semiconductor characteristics. The acceptor concentration (N_A) was obtained by the Mott–Schottky equation [10]:

$$\frac{1}{C^2} = -\frac{2}{e\,\varepsilon\,\varepsilon_0\,N_A\,A^2}\left(V - V_{fb} - \frac{kT}{e}\right) \quad (1)$$

where C represents the capacitance of the space charge region, ε_0 the vacuum permittivity, ε is the dielectric constant of Cu_2O, *e* is the electron charge, *A* is the surface area of the semiconductor/electrolyte interface, *V* is the electrode applied potential, *k* is the Boltzmann constant, *T* is the absolute temperature, N_A is the acceptor concentration and V_{fb} is the flat-band potential of the semiconductor.

According to the M-S relationship, the acceptor density (N_A) can be calculated from the slope of the linear region (figure 4), assuming the dielectric constant of the Cu_2O film is 7.6 in following equation [11]:

$$N_A = -\frac{2}{e\varepsilon\,\varepsilon_0}\left[\frac{d(C^{-2})}{dV}\right]^{-1} \quad (2)$$

The acceptor concentration of Cu_2O_2 is higher than Cu_2O_1, the values calculated being 2.06 x 10^{20} cm^{-3} and 5.08 x 10^{19} cm^{-3}.

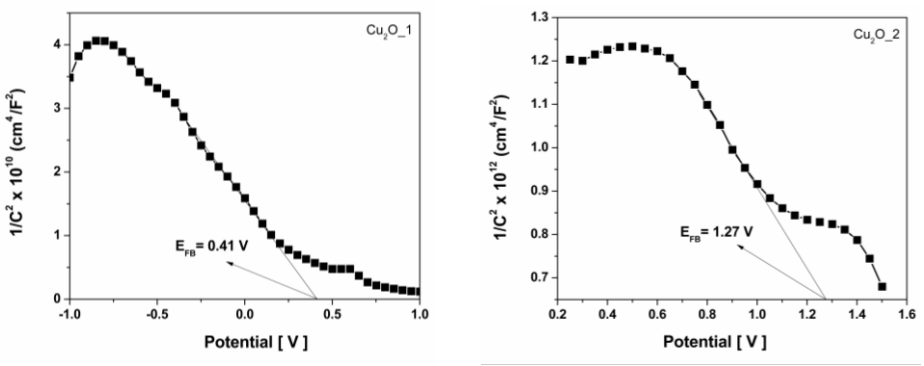

a **b**

Fig. 4. M-S plots of Cu_2O_1 (a) and Cu_2O_2 (b).

It can be observed the positive shift of the flat-band of Cu_2O_2 in figure 4b, which will lead to more positive Fermi level, E_F and thus the higher V_{OC} values in DSSC is expected.

In order to understand the effect of the morphology on the photovoltaic performance of p-type DSSC, the absorption spectra of dye-loaded photocathodes was measured. From figure 5, it can be seen the absorption intensity of Cu_2O_2 is higher than of Cu_2O_1, increasing the photoresponse to visible light for DSSCs.

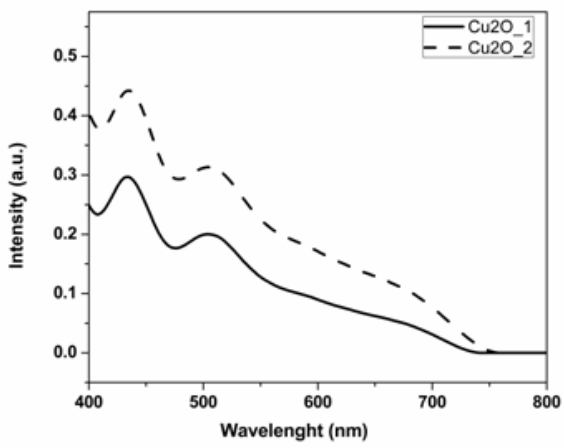

Fig. 5. Absorption spectra of Cu_2O_1 and Cu_2O_2 samples.

Indeed, I-V characteristics of DSSC (Fig. 6) show that the photovoltaic performance has improved in case of the porous structure, showing approximately 15% increase in J_{SC} and V_{OC}.

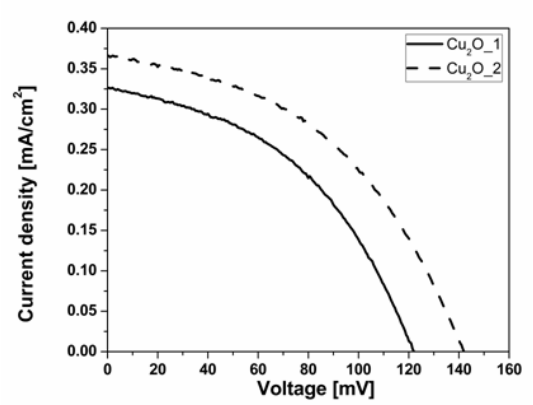

Fig. 6. J-V curve of p-type DSSCs based on Cu_2O_1 and Cu_2O_2 samples.

Electrochemical impedance spectroscopy analysis was performed in order to understand the charge dynamics in both cells (figure 7). The semicircle is evidently larger for Cu_2O_2 cell, indicating that the micrometer porous structure increases the recombination resistance, thus lowering the recombination processes at the oxide/dye/electrolyte interface and increasing the hole lifetime [12].

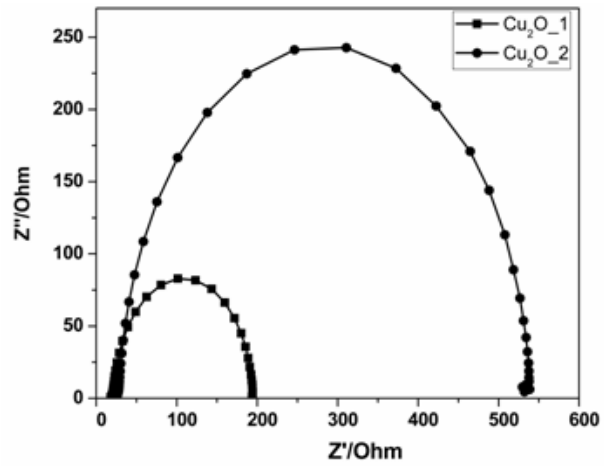

Fig. 7. Impedance spectra of both cells.

4. Conclusions

In summary, cuprous oxide with different morphologies (3D hierarchical structure consisting of the micrometer dendritic rods and the porous truncated octahedrons) has been successfully synthesized via a facile one-step hydrothermal methods using copper (II) acetate and ethyl cellulose as reactants. The p-type DSSC based on the micrometer porous structure exhibits approximately 15% increase in J_{SC} and V_{OC} than 3D hierarchical structure. This enhancement could be explained in that this porous structure is easily loaded with dye molecules and lowering the recombination process at the oxide/dye/electrolyte interface.

For better balancing of surface area, hole transport and light scattering, 3D hierarchical porous structure should be investigated in future works.

Acknowledgements

This work was supported by a grant of the Romanian National Authority for Scientific Research and Innovation, CNCS/CCCDI - UEFISCDI, project number PN-III-P2-2.1-PED-2016-0526, within PNCDI III.

References

[1] S. Mathew, A. Yella, P. Gao, R. Humphry-Baker, B. F. E. Curchod, N. Ashari-Astani, I. Tavernelli, U. Rothlisberger, M. K. Nazeeruddin, M. Gratzel, Nat. Chem. 6 (2014) 242–247

[2] J. Bandara and J. Yasomanee, Semicond. Sci. Technol. 22 (2007) 20-24

[3] T. Jiang, M. Bujoli-Doeuff, Y.Farré, Y. Pellegrin, E. Gautron, M.Boujtita, L. Cario, S. Jobic, F. Odobe, RSC Adv.6 (2016) 112765-112770

[4] K.H. Han, M. Tao. Sol. Energy Mater. Sol. Cells 93 (2009) 153-157

[5] C. Wadia, A. P. Alivisatos, D. M. Kammen. Environ. Sci. Technol. 43 (2009) 2072-2079

[6] S. Ito, P. Chen, P. Comte, M.K. Nazeeruddin, P. Liska, P. Pechy, M. Gratzel, Prog. Photovolt: Res. Appl. 15 (2007) 603–612

[7] R. Ji, W. Sun, Y. Chu. Chemphyschem. 14 (2013) 3971-3976

[8] P. Kubelka. J. Opt. Soc. Am. 38 (1948) 448-457

[9] Y.Yang, D. Xu, Q. Wu, P. Diao. Scientific Reports 6 (2016) 35158-35171

[10] K. Rajeshwar, Fundamentals of Semiconductor Electrochemistry and Photoelectrochemistry, Wiley, New York (2002)

[11] Z.H. Zhang, P.J. Wang. J Mater Chem 22 (2012) 2456–2464

[12] Z-S. Wang, T. Yamaguchi, H. Sugihara, H. Arakawa. Langmuir 21 (2005) 4272–4276.